THE LARGE- AND SMALL-SCALE STRUCTURES OF 3C 293

A. H. BRIDLE[a]
National Radio Astronomy Observatory,[b] VLA Program, P. O. Box 0, Socorro, New Mexico 87801
and Department of Physics and Astronomy, University of New Mexico, Albuquerque, New Mexico 87131

E. B. FOMALONT
National Radio Astronomy Observatory,[b] Charlottesville, Virginia 22901

T. J. CORNWELL
National Radio Astronomy Observatory,[b] VLA Program, P. O. Box 0, Socorro, New Mexico 87801
Received 20 April 1981

ABSTRACT

The radio galaxy 3C 293 has been mapped with the VLA at 1.465 and 15.035 GHz with resolutions of 6″ and 0.″2, respectively, and with the Multi-Element Radio Linked Interferometer Network (MERLIN) at 1.666 GHz with a resolution of 0.″25. The VLA 1.465-GHz map shows that the source has a two-sided Z-shaped structure whose physical association with the galaxy VV 5-33-12 is now clear. The source is unusual in that it is dominated by a steep-spectrum extended core. The core is resolved by the MERLIN 1.666-GHz and VLA 15.035-GHz observations into an inner two-sided structure within 1 kpc of the center of VV 5-33-12, and curved bridges of emission linking this structure to the large-scale emission. If equipartition conditions apply in the core, its straight radio spectrum between 408 MHz and 15 GHz implies that its age since last particle replenishment is less than 5% of the light travel time to the outer radio lobes. The major axis of the core lies 35° from the major axes of the emission bridges that make up the bar of the large-scale Z structure, and 60° from the minor axis of VV 5-33-12. We discuss precessional and buoyant-refraction models for these misalignments. Models based on perturbations of the axis of the primary collimator in 3C 293 appear unattractive, since the galaxy is exceptionally isolated and the required perturbation time scale is short. Models based on continuous-jet refraction in a dense high-temperature core within VV 5-33-12 are plausible, since the required misalignments can be produced by anisotropic pressure gradients in an atmosphere of modest mass and x-ray luminosity. These models may be tested with x-ray observations of the core of VV 5-33-12. If validated, they could explain the tendency of large-scale radio sources to form *near* the minor axes of their associated galaxies.

I. INTRODUCTION

The radio source 3C 293 (= 1350+316) is identified (Wyndham 1965) with the $m_V = 14^m.3$ E6 galaxy VV 5-33-12, whose redshift is 0.0452 (Sandage 1966; Burbidge 1967). The galaxy has several optical and radio peculiarities. An unusually high fraction ($\sim$ 80%) of its radio emission arises in a steep-spectrum ($\alpha \sim 0.7$, $S_\nu \propto \nu^{-\alpha}$) core component several arcseconds in extent around the nucleus of the galaxy (Bridle and Fomalont 1978, hereafter referred to as BF; Argue, Riley, and Pooley 1978, hereafter referred to as ARP). Most of the remaining emission is from a weak extended lobe whose peak is 85″ (52 kpc, $H_0 = 100$ km s^{-1} Mpc^{-1}) northwest of VV 5-33-12. Neither the displacement of the lobe from the galaxy nor the elongation of the lobe itself aligns with the symmetry axes of the extended radio core or of the optical galaxy. The physical association between the extended lobe and the core source has therefore been in some doubt. Reich *et al.* (1980) report weak sources 14′ (510 kpc) and 27′ (980 kpc) from the radio core in approximately the same position angle as the lobe, but their association with the rest of 3C 293 is speculative.

VV 5-33-12 is unusually flat for a radio galaxy and has a complex internal structure (ARP). It has been suggested as a possible Sb by Sandage (1966) and as a possible S0 by Colla *et al.* (1975). Some of the apparent optical complexity is due to dust (Wyndham 1966; Battinisti *et al.* 1980).

The existence of a weak radio bridge between VV 5-33-12 and the extended lobe has been tentatively reported by several observers (Colla *et al.* 1975; Högbom and Carlsson 1974; BF; ARP). The 20-cm map by Högbom and Carlsson in particular suggested that such a bridge might be appreciably linearly polarized. As the existence of an emission bridge would confirm the relationship of the lobe to VV 5-33-12, and its shape could give clues to the origin of the various misalignments present in 3C 293, we made sensitive observations of the source with the VLA (Thompson *et al.* 1980) at 1.465 and 15.04 GHz and with MERLIN (Davies *et al.* 1980) at 1.666 GHz to map both the large- and small-scale structures.

[a] On leave from Queen's University at Kingston, Ontario, Canada.
[b] Operated by Associated Universities, Inc., under contract with the National Science Foundation.

0004-6256/81/091294-12$00.90

TABLE I. Assumed properties of 3C 286.

α(1950.0)	$13^h28^m49^s.657$
δ(1950.0)	30°45′58″.639
Flux density (1.4 GHz)	14.4 Jy
Flux density (15 GHz)	3.4 Jy
Polarization p.a.	33°
Rotation measure	0 rad m^{-2}

II. THE OBSERVATIONS

We observed 3C 293 with 19 antennas of the partially completed VLA on 1 April 1980. Outputs from all antenna pairs were correlated, providing 171 baselines from ~0.1 to ~20 km in length. The source was tracked between H.A. -6^h2 and $+6^h6$, interspersing 13-min observations at 1.465 GHz and 9-min observations at 15.035 GHz with 2-min observations of the nearby calibration sources 1323+321 and 3C 286. The position, flux density, and polarization position angle scales were normalized to the parameters of 3C 286 given in Table I.

Gain and phase fluctuations in the instrument and along the atmospheric path to 1323+321 were monitored as follows. Each 2-min observation of 1323+321 was used to derive the complex gain (amplitude and phase) of every antenna relative to a stable reference antenna. If successive least-squares solutions for the complex gain of a given antenna disagreed in amplitude by more than 10% or in phase by more than 20°, the intervening data for 3C 293 were discarded. This procedure was particularly important at 15.035 GHz for the observations at early and late hour angles during which 3C 293 was at low elevations. After editing of the data using the above criterion, about 100 min of integration on 3C 293 with an average of 16 antennas were used to make the 15-GHz maps.

Intial maps were made from the edited, calibrated data by the usual Fourier methods. These maps were then CLEANed (Högbom 1974). The arrays of δ-function components representing the initial maps were next used as the input models to an algorithm for further fine adjustments of the complex antenna gains implemented at NRAO by Schwab (1980). This algorithm uses the model to predict the visibility amplitudes and phases to be expected on all interferometer pairs throughout the observations, and adjusts the complex antenna gains as functions of time to minimize the discrepancies between the observed and predicted visibilities. This procedure, termed "self-calibration," is rapidly convergent for a multielement array such as the VLA. It is equivalent to the "hybrid mapping" procedure used in very-long-baseline interferometry (e.g., Readhead and Wilkinson 1978).

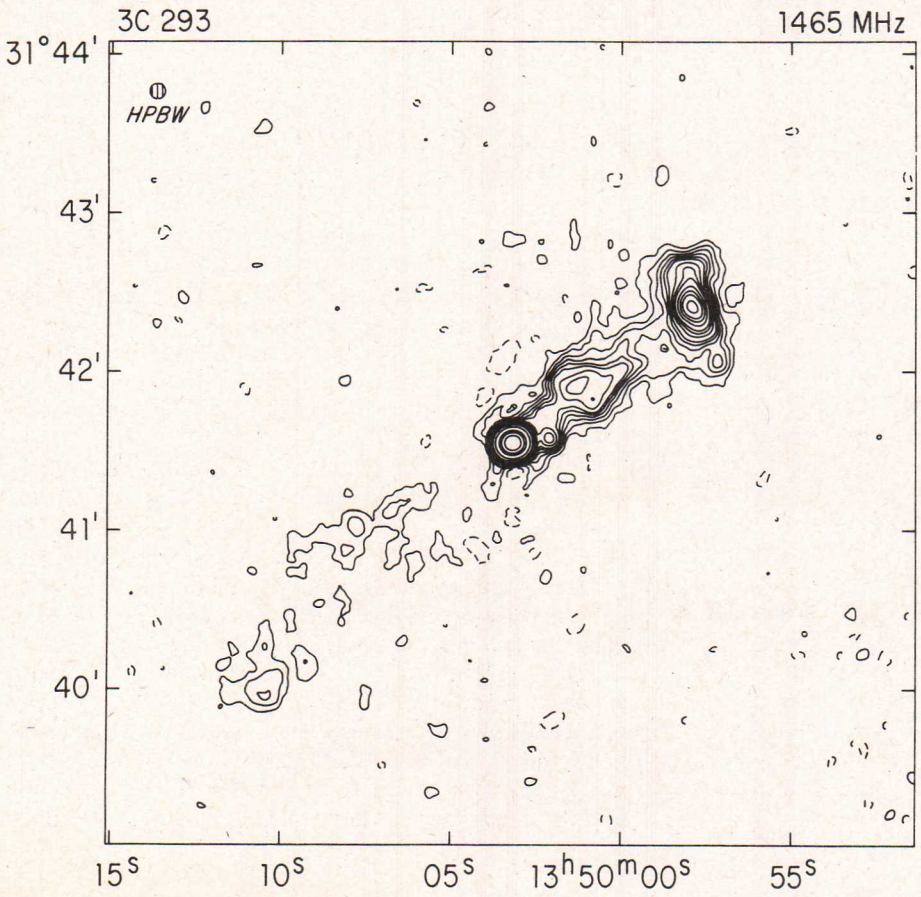

FIG. 1. Contours of total intensity over 3C 293 at 1.465 GHz, resolution (FWHM) 6″.0 in each coordinate. Contours are drawn at 2, 4, 6, 8, 10, 12, 16, 20, 24, 32, 40, 48, 60, 80, and 200 mJy/beam. The peak intensity on the map is 3.25 Jy. The HPBW is indicated by the shaded circle at the upper left.

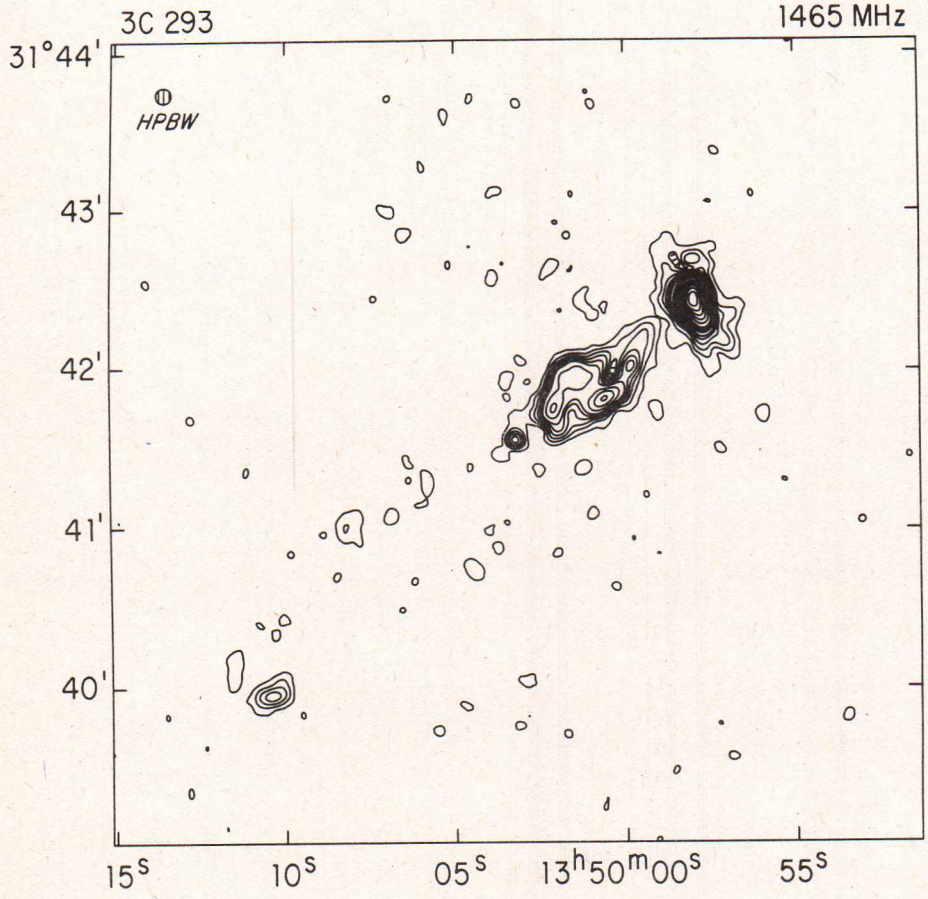

FIG. 2. Contours of linearly polarized intensity over 3C 293 at 1.465 GHz, resolution as in Fig. 1. Contours are drawn at 0.4, 0.8, 1.2, 1.6, 2.0, 2.4, 3.2, 4.0, 4.8, 6.4, 8.0, 9.6, 11.2, and 12.8 mJy/beam. The peak intensity on the map is 13.9 mJy. The HPBW is indicated by the shaded circle at the upper left.

Additional observations of the small-scale structure of 3C 293 were made on 8 August 1980 with the partially completed Multi-Element Radio Linked Interferometer Network (MERLIN) at Jodrell Bank. The five telescopes then in the network provided ten baselines ranging from ~8 to ~133 km in length. At the observing frequency of 1.666 GHz the maximum resolution is 0".25. 3C 293 was tracked for all hour angles between -7^h and $+8^h$. Flux density calibration is somewhat difficult at this frequency and resolution because most nonvariable calibrators are slightly resolved. We therefore used the source BL Lac to establish the calibration of each baseline, and short-baseline data on 3C 48 and 3C 147 to establish the overall flux density calibration (on the Baars *et al.* 1977 scale). This procedure removes long-term baseline-related effects, such as correlator errors. No short-term calibration of the telescope complex gains was made during these observations. Instead, a self-calibration algorithm (Cornwell and Wilkinson 1981) similar to that used on the VLA data was employed. Consequently, the absolute position of the 1.666-GHz map is unknown and has to be inferred from comparison with the VLA data. (The position scale on the VLA maps is determined by the initial calibrations relative to 1323+321 and 3C 286 prior to self-calibration.)

III. THE LARGE-SCALE STRUCTURE OF 3C 293

Figure 1 shows a self-calibrated map of 3C 293 at 1.465 GHz with a circular beam of HPBW 6". This map was obtained by applying a Gaussian tapering function falling to $1/\sqrt{e}$ at 4 km from the VLA center. The lowest contour is drawn at 2 mJy/beam while the peak on the map is 3250 mJy/beam. The use of the self-calibration algorithm is primarily responsible for the high (> 1500:1) dynamic range achieved in this map.

The map clearly delineates a broad emission bridge extending northwest from the core component along p.a. 128° and terminating in the extended lobe 85" (52 kpc) from the core. The presence of this bridge confirms the physical association between the core and the lobe beyond any reasonable doubt.

The map also shows a weaker emission bridge extending for abut 130" (79 kpc) southeast from the core along p.a. 121°. This bridge also terminates in an enhanced patch of emission, or lobe. Our detection of the additional weak radio features to the southeast of VV 5-33-12 shows that the overall low-level radio emission associated with the galaxy is a large-scale Z shape with arms of

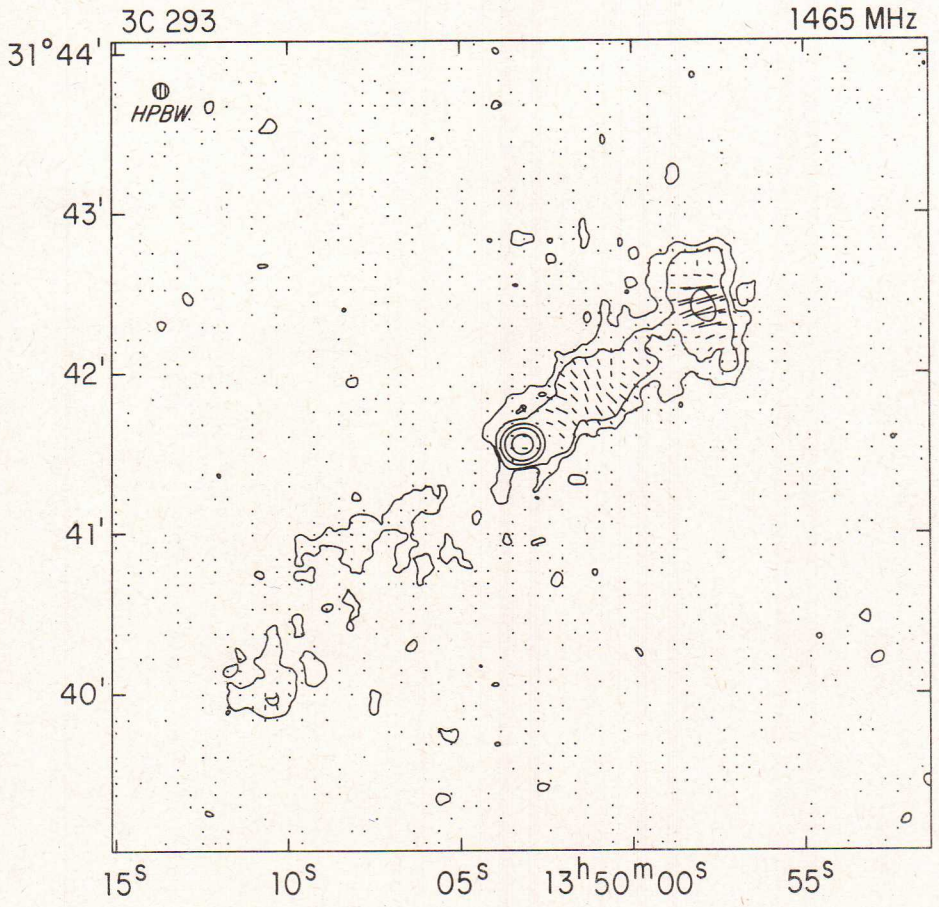

FIG. 3. Distribution of position angles of linearly polarized intensity over 3C 293 at 1.465 GHz, resolution as in Fig. 1. The lengths of the vectors are proportional to the polarized intensity and their angles are those of the observed E vectors. The 2-, 6-, 40-, and 200-mJy/beam contours from Fig. 1 are shown for reference. The HPBW is indicated by the shaded circle at the upper left.

unequal length and brightness. The southeastern structure cannot be an artifact of the calibration process, since its linear scale is approximately 40% larger than that of the northwestern emission and it does not lie along the same position angles as the northwestern structure.

Discovery of the weak *two*-sided structure in 3C 293 removes one of the peculiarities attributed to the source by ARP, namely its apparent one-sidedness in maps of poorer sensitivity and dynamic range. A remaining radio peculiarity of the system is the unusually high brightness contrast between the extended structure and its central extended core. In this respect, 3C 293 more closely resembles sources with dominant small-diameter cores and weak extended emission associated with some powerful radio galaxies and quasars (Perley, Fomalont, and Johnston 1980, 1981). However, 3C 293 differs from these sources in two respects. First, it is identified with a relatively nearby galaxy and is therefore a relatively low-luminosity source. Second, its core has a transparent radio spectrum with index $\alpha \sim 0.7$ (see Table III in Sec. IV), whereas the compact cores in the sources studied by Perley *et al.* generally have flat radio spectra ($\alpha \sim 0$).

Figure 1 shows that the emission bridge to the northwest has a complicated internal structure in that the ridge line of the emission does not lie along the geometrical center of the bridges, but oscillates around it with a "wavelength" of order 30″ (18 kpc). This effect is more prominent in the map of polarized intensity $P = (Q^2 + U^2)^{1/2}$ at this frequency and resolution, shown in Fig. 2.

The central one is $< 1\%$ linearly polarized at 1.465 GHz, but the bridge emission has degrees of polarization reaching 40% at several locations along its edges. The degree of polarization in the northwestern lobe tends to increase from the southwestern edge of the lobe toward the northeastern, taking values from 15% to 18% in the southwest and 22% to 26% in the northeast. In general, the peaks of total intensity along the northwestern bridge are less strongly polarized than the fainter regions, i.e., the polarized intensity varies less along the bridge than does the total intensity. In this respect, the bridge emission in 3C 293 resembles the long linear jet in NGC 315 (Willis *et al.* 1981).

Figure 3 shows the distribution of the position angle of the linear polarization over the source at the same resolution as in Figs. 1 and 2. The E vectors tend to lie at right angles to the ridge line of the polarized intensity distribution; the change in position angle between the bridge emission and the lobe is particularly striking. As the Faraday rotations of these vectors are not known, we

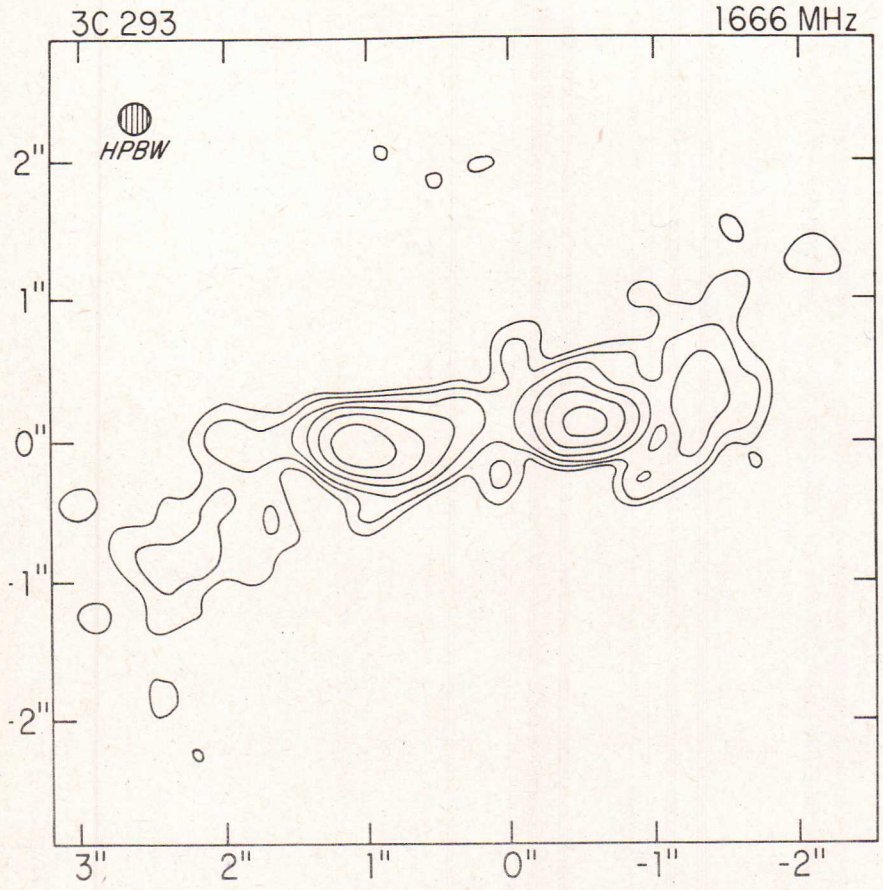

FIG. 4. Contours of total intensity over the core region of 3C 293 at 1.666 GHz, resolution (FHWM) 0".25×0".25. Contours are drawn at 4.4, 8.8, 17.6, 35.2, 70.5, 141, and 282 mJy/beam. The peak intensity on the map is 568 mJy.

cannot infer the orientation of the magnetic field in either the bridge or the lobe from these data.

IV. THE FINE STRUCTURE IN THE RADIO CORE

Figure 4 shows the 1.666-GHz MERLIN map of the core source at 0".25×0".25 HPBW. The core is resolved into two inner components in p.a. ~90°, plus more extended emission. The inner components correspond to the "extended core" previously detected by BF and ARP.

The outer extensions of the core structure on the MERLIN map curve towards the position angle of the large-scale bridges (Figs. 1–3). The southeastern extension is also clearly seen on a VLA 15.035-GHz map tapered to 0".76×0".67 HPBW (Fig. 5). The northwestern extension on the MERLIN map blends with the western component of the core in this VLA map.

Figure 6 shows a map of the inner core structure at 0".24×0".18 HPBW (major axis in p.a. 119°) obtained by tapering the self-calibrated 15.035-GHz VLA data with a Gaussian falling to $1/\sqrt{e}$ at 15 km from the array center. The central double structure shown by the MERLIN map and the earlier maps of BF and ARP is here resolved into several subcomponents. The positions, flux densities, and intrinsic angular sizes of the components of a four-component Gaussian model fitted to the VLA visibility data are listed in Table II. Most of this emission lies within 1".5 (900 pc) of the center of the galaxy.

This inner core structure is approximately perpendicular to a dust lane in the nuclear region of VV 5-33-12, shown by Battinisti *et al.* (1980, their Fig. 4d). Note that their plate is printed with south to the top and west to the right. The alignment of the inner structure of 3C 293 with respect to this dust lane therefore conforms to the correlation between the radio axis and the dust distribution found for seven other radio galaxies by Kotanyi and Ekers (1979). In Sec. VI, we consider models for the misalignment of the *large*-scale radio structure with the inner radio core and with the optical axes of VV 5-33-12.

The cross in Fig. 6 marks the position of the center of VV 5-33-12 measured to ~1" accuracy by ARP. This position suggests that the radio core is a "miniature double" radio source with a weak bridge leading to the center of the galaxy. Both the placement of the core emis-

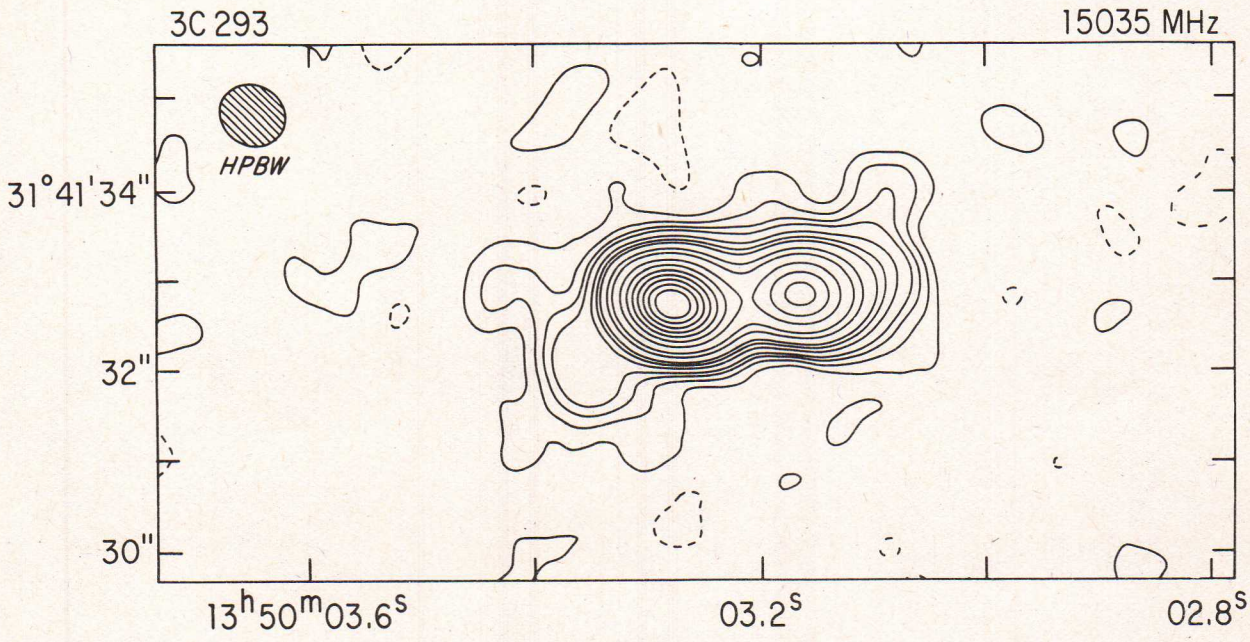

FIG. 5. Contours of total intensity over the core region of 3C 293 at 15.035 GHz, resolution (FWHM) 0".76×0".67, major axis in p.a. 63°. Contours are drawn at −1%, 1%, 2%, 3%, 4%, 6%, 8%, 10%, 15%, 20%, 30%, 40%, 50%, 60%, 70%, 80%, and 90% of the peak intensity of 324 mJy/beam. The HPBW is indicated by the shaded ellipse at the upper left.

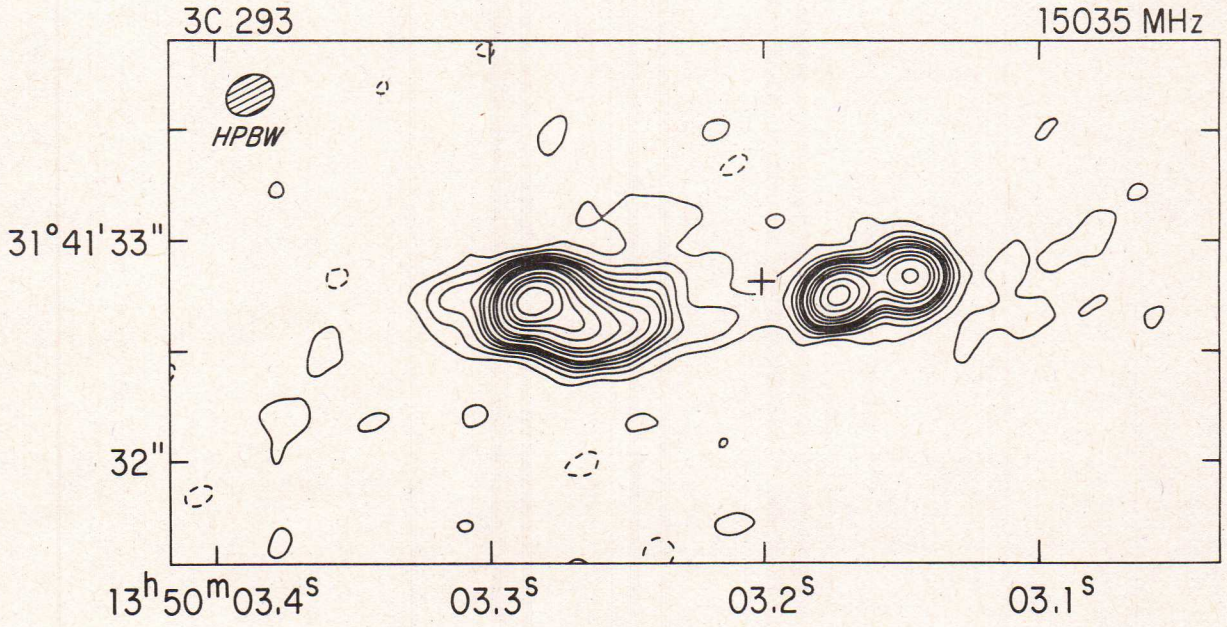

FIG. 6. Contours of total intensity over the core region of 3C 293 at 15.035 GHz, resolution (FWHM) 0".24×0".18, major axis in p.a. 119°. Contours are drawn at −4, 4, 8, 12, 16, 24, 32, 40, 48, 64, 80, 96, and 120 mJy/beam. The peak intensity on the map is 151 mJy. The HPBW is indicated by the shaded ellipse at the upper left.

TABLE II. Parameters of core region of 3C 293.

		(a) 15-GHz compact core components from Gaussian model [a]		
A	91 ± 14 mJy	$13^h50^m03^s.15$	31°41′32″.9	(0″.16×0″.08 in p.a. 38°)
B	109 ± 12 mJy	$13^h50^m03^s.17$	31°41′32″.8	(0″.13×0″.08 in p.a. 88°)
C	316 ± 38 mJy	$13^h50^m03^s.27$	31°41′32″.7	(0″.61×0″.20 in p.a. 83°)
D	101 ± 10 mJy	$13^h50^m03^s.28$	31°41′32″.8	(0″.05×0″.03 in p.a. 95°)
		(b) 1.47-GHz core Gaussian model [a]		
	3.61 ± 0.07 Jy	$13^h50^m03^s.21$	31°41′32″.7	(2″.5×0″.6 in p.a. 103°)
		(c) Position of brightest optical knot (ARP)		
		$13^h50^m03^s.20$	31°41′32″.8	

[a]Integrated flux density, 1950.0 peak position, deconvolved FHWM.

sion relative to this optical position and the morphology of the radio core itself suggest that the core is not an asymmetric one-sided "core-jet" structure such as those detected by VLBI observations of *flat*-spectrum compact cores in several radio galaxies (e.g., Linfield 1981; Preuss *et al.* 1981). It is clearly desirable to obtain a more accurate position for the optical center of VV 5-33-12, however, to improve the relative registration of radio and optical images of the core of the galaxy.

The only significant linearly polarized emission in the core at 15.035 GHz occurs near the peak of the eastern emission in Fig. 6 (components C and D of Table II). The degree of linear polarization there is ~25%. Assuming that the Faraday rotation is small at this high frequency, the magnetic field in the eastern part of the core appears to be circumferential (as in many large-scale radio lobes) rather than parallel to the elongation of the structure (as in the bases of the large-scale radio jets).

Table III lists the integrated spectrum of the core, compiled from the measurements made by BF, by ARP, and in this paper (VLA data). The spectrum is consistent with a single power law of index 0.7 from 408 MHz to 15.035 GHz. There may, however, be spectral differences within the core. The ratio of brightnesses in the eastern and western emission regions in the lower-resolution 15.035-GHz VLA map (Fig. 5) is 2:1, whereas that in the 2.7-GHz map of BF is 1.23:1 and that on the MERLIN 1.666-GHz map (Fig. 4) is almost 1:1. These differences could be explained if the small-diameter component D in Table II had a significantly flatter spectrum than the other core emission, so that the lower-frequency maps are dominated by component C. However, high-resolution maps of the core at intermediate frequencies are required to substantiate this.

V. PHYSICAL CONDITIONS IN THE SOURCE

Table IV lists equipartition parameters for various regions of the core and the bridges in 3C 293. These parameters were calculated assuming (a) that the radio spectra are power laws with the given indices from 10 MHz to 100 GHz and (b) that equal energies reside in relativistic electrons and protons.

The equipartition magnetic field strengths in the core components range from 6×10^{-4} to 3×10^{-3} G. In a field of strength 10^{-3} G the synchrotron half-life of particles radiating at 15 GHz is 8600 yr. The time since last reacceleration of these particles in the core of 3C 293 must therefore be significantly less than 10^4 yr since there is no evidence for high-frequency steepening of the spectrum of the core (Table III). Furthermore, the light travel times over the projected distance from the core to the preceding and following lobes are 1.7×10^5 and 2.6×10^5 yr, respectively. The time since the last reacceleration of radiating particles in the core components must therefore be much less than 5% of the kinematic

TABLE III. Integrated spectrum of 3C 293 core.

Frequency (MHz)	Observed flux density (Jy)	Fitted [a] flux density (Jy)	Reference
408	8.9	8.83	ARP
1407	3.75	3.70	ARP
1465	3.61 ± 0.07	3.60	This paper
2695	2.4	2.35	ARP
2695	2.40 ± 0.08	2.35	BF
4995	1.36	1.52	ARP
8085	1.03 ± 0.04	1.09	BF
15000	0.55	0.70	ARP
15035	0.75 ± 0.05	0.70	This paper

[a]Power-law spectrum $S(\nu)\sim\nu^{-0.70}$.

TABLE IV. Equipartition parameters in 3C 293.[a]

Location	Adopted spectral index	Magnetic field strength (G)	Minimum energy density (J cm^{-3})	Confining nT (cm^{-3} K)
Core (A)	0.7	1.1×10^{-3}	1.1×10^{-8}	2.7×10^{8}
Core (B)	0.7	1.2×10^{-3}	1.3×10^{-8}	3.3×10^{8}
Core (C)	0.7	6.1×10^{-4}	3.5×10^{-9}	8.9×10^{7}
Core (D)	(a) 0.7	2.7×10^{-3}	6.7×10^{-8}	1.7×10^{9}
	(b) 0.0	1.9×10^{-3}	3.2×10^{-8}	8.2×10^{8}
NW bridge (8.4 kpc)	0.7	1.6×10^{-5}	2.4×10^{-12}	6.1×10^{4}
NW bridge (12 kpc)	0.7	1.1×10^{-5}	1.0×10^{-12}	2.6×10^{4}
NW bridge (20 kpc)	0.7	1.0×10^{-5}	9.9×10^{-13}	2.5×10^{4}
NW bridge (28 kpc)	0.7	1.0×10^{-5}	9.8×10^{-13}	2.5×10^{4}
NW bridge (41 kpc)	0.7	8.3×10^{-6}	6.5×10^{-13}	1.6×10^{4}
NW lobe peak	0.7	1.5×10^{-5}	2.2×10^{-12}	5.6×10^{4}
SE bridge (40 kpc)	0.7	1.7×10^{-5}	2.7×10^{-12}	6.8×10^{4}

[a]Assuming fully filled cylindrical volume with depth equal to FHWM transverse to major extent in plane of sky, power-law spectra from 10 MHz to 100 GHz, and equal energies in electrons and protons.

age of the large-scale structure.

Thermal pressures equivalent to nT in the range 10^8–10^9 cm^{-3} K would be required to confine the minimum energy densities in the core components. These components are therefore unlikely to be confined by gas at temperatures near 10^4 K that would be typical of optical line-emitting regions near galactic nuclei, unless the gas in 3C 293 is exceptionally dense. If the core components are confined at all by external thermal pressure, the confining medium is more likely to be gas at temperatures of order 10^8 K, more typical of the effective temperatures of extended x-ray sources associated with some active galaxies.

The equipartition magnetic field strengths in the bridges and the lobes of 3C 293 are of order $(1–2)\times10^{-5}$G. These field strengths are sufficiently low that the particles radiating at 1.4 GHz in the bridges need not be reaccelerated there unless the velocity of particle transfer from the core is less than $0.01c$. Observations of the bridges at 4.9 GHz are planned in order to place stricter constraints on this argument. The thermal pressures that would be required to confine the minimum energy densities in the bridges and in the lobes correspond to nT products in the range $(1.6–6.8)\times10^4$ cm^{-3} K. X-ray observations of 3C 293 should therefore be able to test whether these structures are thermally confined. We note that the energy density in the lobes is only 1–3 times that in the bridges if both are in equipartition, so it is possible that the lobes are simply extensions of the bridge structure viewed at different angles to the line of sight.

VI. MODELS FOR THE MISALIGNMENTS WITHIN 3C 293

Figure 1 shows that the overall bridge-and-lobe morphology of 3C 293 is Z shaped, and Figs. 1 and 4 taken together show that the inner core structure (p.a. ~90°) is misaligned with both the northwestern bridge (p.a. 128°) and the southeastern (p.a. 121°) and with the optical minor axis of VV 5-33-12 (p.a. ~150°). Figure 4 itself shows that the outer core structure approaches the position angles of the bridges within a few kiloparsecs of the centroid of the core.

We consider two types of interpretation for these misalignments. The first, based on precession of a central collimator, is not strongly supported by the new radio observations. The second, based on refraction of a continuous jet by pressure gradients in a confining medium, is consistent with our data and may be tested using high-resolution x-ray observations.

a) Misalignment by Precession of the Collimator

Several authors have suggested that Z symmetry in large-scale extragalactic radio sources may be due to precession (or, more generally, to secularly changing orientation) of the primary collimators of such sources (e.g., Bridle *et al.* 1976; Miley 1976; Ekers *et al.* 1978; Rees 1978; Lonsdale and Morison 1980). This interpretation is particularly attractive for large sources whose lobe structures themselves show evidence for curvature with rotational symmetries (e.g., NGC 326, Ekers *et al.* 1978; 3C 196, Lonsdale and Morison 1980; 3C 315, Högbom 1979). In the absence of firm constraints on particle lifetimes in the lobes from observations of radio spectral gradients across them, it is difficult to constrain dynamical models for such rotationally symmetric structures.

In the case of 3C 293, the only constraints we have on precessional models are the nature and scale of the internal misalignments, since the lobes are of small transverse extent and the bridges are sensibly straight. Possible evidence against a precessional interpretation of the large-scale Z symmetry of this source is the 35° misa-

lignment between the inner core and the bridges. If the Z symmetry is attributed to rotation of the central collimator from north toward west over the lifetime of the source, it is surprising that the inner ~2-kpc core "leads" the bridges by as much as 35° in this rotation.

If the 35° misalignments between the core and the bridges were attributed to a perturbation of the primary collimator in 3C 293 during the last 10^4 yr, it is not clear what agency could be responsible for the perturbation. It has been suggested (e.g., Rees 1978) that galaxy-galaxy interactions might produce the angular displacements seen in several radio structures with *large-scale* rotational distortions (e.g., NGC 326, 3C 315) and these sources are indeed identified with galaxies having close companions of comparable brightness. The time scale associated with galaxy-galaxy interactions should however be $\gg 10^4$ yr.

Even if we have significantly underestimated the time scale for particle replenishment in the core (e.g., by overestimating the magnetic field strength there), it is unlikely that the misalignments in 3C 293 have resulted from galaxy-galaxy interactions, since VV 5-33-12 is in a region of unusually low galactic density (Stocke 1979). Although it is within the boundaries in the Zwicky and Herzog (1963) catalog of two clusters (1350.0+3148 and 1352.0+3107), it is unlikely to be associated with either of them. The first is a "very distant" ($0.15 < z < 0.2$) cluster, while the redshift of VV 5-33-12 is only 0.0452. The center of the second cluster is about 50′ from VV 5-33-12, and the ratio of this separation to the cluster radius makes it unlikely that 3C 293 is in the cluster according to the statistics presented by Burns and Owen (1977). The only optical object that might be a close companion to VV 5-33-12 is a spherical diffuse image ~3 m fainter than the galaxy and ~30″ west and ~15″ south of its nucleus (ARP). It is not clear whether this is a faint companion to VV 5-33-12, a bright knot in its envelope, or a background object. In any of these cases it would be surprising if it had produced a major perturbation of the central collimator of 3C 293, as it is so much fainter than the galaxy. This apparent isolation of VV 5-33-12 leads us to prefer other interpretations for the 35° misalignment between the core and the bridges, which we discuss below.

The oscillations of the *ridge line* of the northwestern bridge, especially those seen in the polarized-intensity map (Fig. 2), could be fitted to helical geometries such as those used to interpret the time-variable radio structure of SS 433 (Hjellming and Johnston 1981). Attempts to fit this ridge-line structure by assuming the presence of a precessing collimator in 3C 293 would, however, be forced to postulate a large recent perturbation of the collimator in order to explain the present orientation of the inner radio core. Such models would therefore be subject to the same difficulties as those discussed above for precessional models of the large-scale Z symmetry. It may be more attractive to interpret the ridge-line oscillation of the northwestern bridge as a growing helical instability in a jet whose collimator remains fixed in space (Hardee 1979). The final swings of such an instability could then be responsible for the deflections at the ends of the bridges which form the lobe-like structure. In such a model the Z symmetry would be an accident resulting from differing growth rates of the instability on the two sides of the structure.

b) Refraction in a Confining Atmosphere

A mechanism for producing large-scale S-shaped distortions of radio galaxies by buoyant refraction of light "bubbles" encountering pressure gradients in dense circumgalactic atmospheres was proposed by Gull and Northover (1973) and by Harris (1974). This mechanism suffered from the difficulty that implausibly long time scales were required for transport of the bubbles over typical radio source sizes, since the bubble velocities in this model would be only a few hundred km s^{-1}. The mechanism we consider here is the continuous-jet analog of the buoyancy model of Gull and Northover, introduced by Henriksen, Vallée, and Bridle (1981, hereafter referred to as HVB).

There is growing evidence from observations of C-shaped (head-tail) radio galaxies in clusters that continuous jets of radio emission can be bent through angles approaching 90° without disruption by *dynamic* pressure gradients. [See, for example, the recent VLA maps of NGC 1265 (Owen *et al.* 1978), 1638+537 (Burns and Owen 1980), and IC 708 (Vallée, Bridle, and Wilson 1981).] Models for the response of continuous jets to the pressure gradients resulting from translation of the parent galaxy through a circumgalactic medium have been developed by Begelman *et al.* (1979) and by Jones and Owen (1979). The recent discoveries of dense high-temperature atmospheres of some massive elliptical galaxies (e.g., Fabbiano *et al.* 1979; Fabricant *et al.* 1978, 1980) make it attractive to postulate (HVB) that jets will be similarly stable while bending under the influence of *static* pressure gradients within such high-temperature galactic atmospheres. As HVB give a general treatment of such buoyant *jet* refraction, only the principle necessary for an illustrative application to 3C 293 is outlined here.

Suppose that a radio jet emerges from a collimating "nozzle" at an angle i to the minor axis z of a surrounding pressure distribution $p(x,y,z)$. This hypothesis is particularly attractive for 3C 293 as the radio core is misaligned by 60° to the minor axis of the large-scale structure of an exceptionally flat galaxy. Take coordinates such that the jet is formed in the (y,z) plane. The jet will bend (HVB) with an instantaneous radius of curvature R in this plane given by

$$\frac{\rho_j V_j^2}{R} = \frac{\partial p}{\partial z} \sin i + \frac{\partial p}{\partial y} \cos i, \qquad (1)$$

where ρ_j and V_j are the density and velocity of the material flow in the jet and the weight of the jet has been

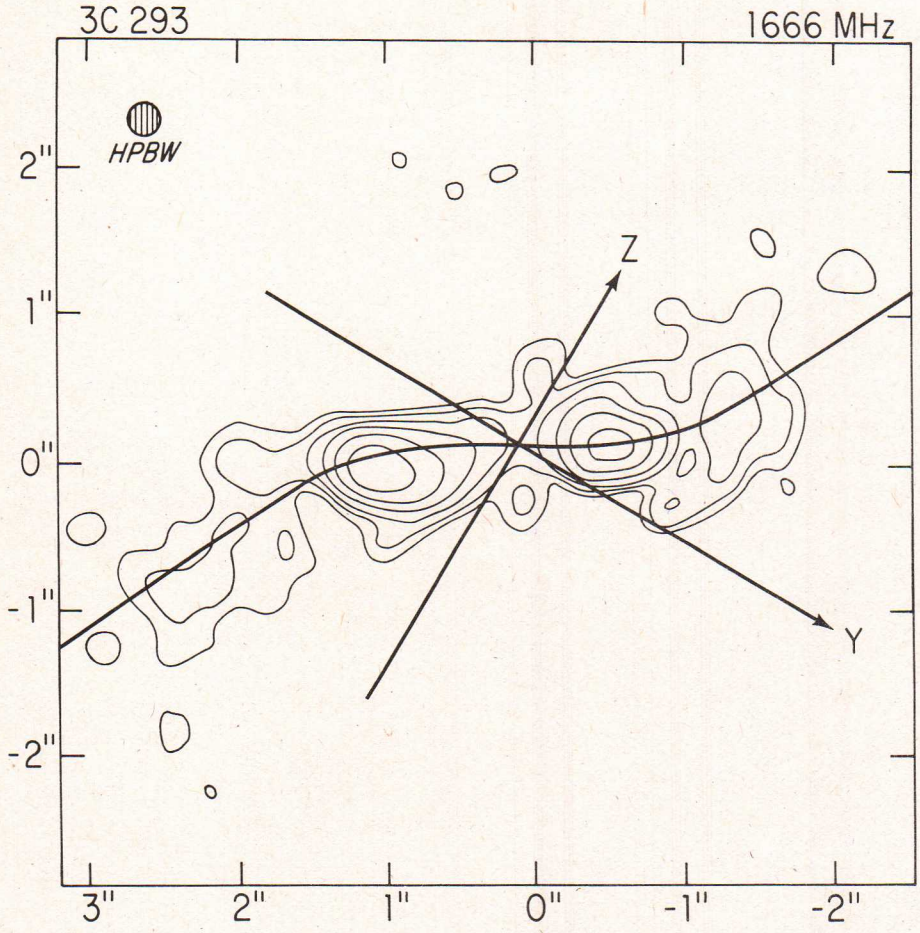

FIG. 7. The curved trajectory of the refracted-jet model described in Sec. V b superposed on the MERLIN 1.666-GHz map from Fig. 4. The z axis is the minor axis of VV 5-33-12. The asymptotic position angles of the trajectory are the mean position angle of the northwestern and southeastern bridges from Fig. 1.

neglected. In the case of 3C 293, we know that $i \sim 60°$ and that $R \sim 500$ pc in the outer core. Furthermore, the condition $p \sim \rho_j V_j^2$ is required for nozzle formation and is therefore likely to hold in regions of the jet that are not far from the nozzle. Given an *assumed* pressure distribution $p(x,y,z)$, Eq. (1) can be solved for the trajectory of the jet. (Explicit solutions for two pressure distributions of general interest are given by HVB.)

To estimate the magnitude of the parameters needed to produce the inner 35° curvature in 3C 293, we consider the jet to be formed at the geometrical center of an isothermal spheroidal density distribution in the form

$$n(x,y,z) = n_0 \Big/ \left[1 + \left(\frac{x^2+y^2}{a^2} + \frac{z^2}{b^2}\right)^c\right], \qquad (2)$$

where a and b are the major and minor axis lengths of the spheriod, c is a scaling parameter, and n_0 is the central density. Numerical integration of (1) with this density distribution gives a trajectory that is an acceptable fit to the core structure in Figs. 4 and 5, and to the subsequent 25° misalignment between the bridges and the minor axis of the galaxy (taken as the z axis) if the adjustable parameters in (2) are $a = 650$ pc, $b = 410$ pc, and $c = 4$. The fit to the MERLIN data is shown in Fig. 7. We have assumed for simplicity that the (y,z) plane is the plane of the sky, and the parameters of this fit should be regarded as illustrative rather than unique. The fitted density distribution (2) falls off rapidly beyond the region of the inner radio core, so the motion of the jet is not significantly influenced by this distribution on the scale of the bridge structure in Fig. 1. This is the main reason that the bridges do not lie along the minor axes of the galaxy in this model.

The scaling density n_0 in (2) can be estimated if we assume a temperature for the confining atmosphere, by requiring that the pressure confine the minimum energy densities estimated for the core components in Table IV. Given an assumed temperature, the total mass of confining gas can be obtained by integrating (2) over all space. We can also predict the thermal bremsstrahlung luminosity of the gas distribution by using (2) with the expression

$$L_X(E_1,E_2) = 1.995\times10^{-27} g T^{1/2} \times [\exp(-E_1/kT) - \exp(-E_2/kT)] \times \int n^2\, dV, \qquad (3)$$

for the luminosity L_X in erg s^{-1} between energies E_1 and E_2 at temperature T. Equation (3) is obtained by integrating the bremsstrahlung emissivity (Allen 1973)

TABLE V. Expected 0.5–4-keV luminosities of gaseous spheroids required by refraction model for 3C 293 core misalignment (erg s^{-1}).

Assumed temperature	10^7 K	$10^{7.5}$ K	10^8 K	$10^{8.5}$ K
Central density $n_0 = 10^0$ cm^{-3} Total mass $= 2.3\times10^7$ $M_\odot$	uc	uc	1.3×10^{41}	8.7×10^{40}
Central density $n_0 = 10^{0.5}$ cm^{-3} Total mass $= 7.3\times10^7$ $M_\odot$	uc	1.4×10^{42}	1.3×10^{42}	8.7×10^{41}
Central density $n_0 = 10^1$ cm^{-3} Total mass $= 2.3\times10^8$ $M_\odot$	7.2×10^{42}	1.4×10^{43}	1.3×10^{43}	oc
Central density $n_0 = 10^{1.5}$ cm^{-3} Total mass $= 7.3\times10^8$ $M_\odot$	7.2×10^{43}	1.4×10^{44}	oc	oc
Central density $n_0 = 10^2$ cm^{-3} Total mass $= 2.3\times10^9$ $M_\odot$	7.2×10^{44}	oc	oc	oc

Notes to Table V

uc—unacceptable model, core components would be unconfined.
oc—unacceptable model, core components would be overconfined.
X-ray luminosity of M87—2×10^{43} erg s^{-1}.

over energy, solid angle, and the source volume, putting $\Sigma Z^2 n_e n_i = 1.4n^2$ for a plasma with cosmic abundances (Tucker 1975); g is the effective Gaunt factor in the energy range (E_1,E_2). Table V gives central densities, total masses, and 0.5–4.5-keV luminosities for model atmospheres capable of producing the observed core-bridge misalignment in 3C 293, for various assumed temperatures.

For temperatures $T \lesssim 10^8$ K, the required atmospheric component would be a powerful x-ray source, but the luminosity implied by the model is a strong function of the assumed temperature. Observations of the temperature and luminosity of the core of VV 5-33-12 at x-ray energies should therefore place important constraints on the refracted-jet model for the radio structure of 3C 293.

VII. CONCLUSIONS

The new VLA and MERLIN maps of 3C 293 show beyond reasonable doubt that the previously detected "one-sided lobe" is indeed physically associated with the active galaxy VV 5-33-12 and that the source is in fact a large-scale *two*-sided Z-shaped structure with an unusually dominant steep-spectrum extended core. The physical conditions in the core imply that the replenishment of its radiating particles has occurred relatively recently in the history of the radio structure. Its 35° misalignment with the large-scale emission bridges and its 60° misalignment with the minor axis of the galaxy are consistent with interpretation of both misalignments as due to refraction of a collimated radio jet by static pressure gradients in a hot dense atmospheric core within the galaxy, whose minor axis is aligned with that of the light distribution in VV 5-33-12. The nature of the ridge-line oscillations along the brighter bridge, the relationship of the bridge to the lobe structure, and the magnetic field configuration in the bridge cannot be inferred from these single-frequency observations.

If the jet refraction model discussed for 3C 293 in Sec. VI b is validated by future x-ray observations, it could be applied to explain why large-scale radio sources appear to lie preferentially near the projected minor axes of their associated galaxies (Palimaka *et al.* 1979). The degree of alignment of the *outer* part of a radio jet with the minor axis of the high-temperature component of its parent galaxy's atmosphere would depend on both the *steepness* and the *anisotropy* of the atmospheric pressure gradients $\partial p/\partial y$ and $\partial p/\partial z$. Good alignment with the minor axis of this atmosphere would be obtained if a and b in (2) differed significantly and if the pressure gradients can produce the realignment before the pressures fall below those which are able to bend the jet trajectory significantly. A minor axis *preference* (rather than a perfect correlation) such as that found by Palimaka *et al.* (1979) is to be expected if the inclination angles i of the primary collimators to the minor axes of the galactic atmospheres are in fact widely distributed and if the axial ratios of different radio-galaxy atmospheres vary widely. The mechanism may also operate on still smaller scales to account for the tendency of radio core structures to form at right angles to dust lanes in radio galaxies, if these dust lanes are associated with dense and highly flattened gaseous disks. It could therefore also offer an explanation for the correlation between radio axes and dust lane orientations found by Kotanyi and Ekers (1979). Observations of the orientations of the outer parts of radio jets relative to the minor axes of any extended x-ray emission associated with their parent radio galaxies will provide a powerful test of these hypotheses.

We thank Professor R. N. Henriksen for discussions on the dynamics of jets, and Dr. J. P. Vallée for an early version of the numerical routine used to calculate jet trajectories. A.H.B. thanks the National Radio Astronomy Observatory and the University of New Mexico for their hospitality during a sabbatical leave from Queen's University at Kingston during which this work was completed. This research was partially supported by a grant to A.H.B. from the Natural Sciences and Engineering Research Council of Canada. T.J.C. gratefully acknowledges receipt of a United Kingdom Science Research Council postdoctoral research fellowship.

REFERENCES

Allen, C. W. (1973). *Astrophysical Quantites* (Athlone, London), p. 103.
Argue, A. N., Riley, J. M., and Pooley, G. G. (1978). Observatory **98**, 132 (ARP).
Baars, J. W. M., Genzel, R., Pauliny-Toth, I. I. K., and Witzel, A. (1977). Astron. Astrophys. Suppl. **61**, 99.
Battinisti, P., Bonoli, F., Silvestro, S., Fanti, R., Gioia, I. M., and Giovannini, G. (1980). Astron. Astrophys. **85**, 101.
Begelman, M. C., Rees, M. J., and Blandford, R. D. (1979). Nature **279**, 770.
Bridle, A. H., Davis, M. M., Meloy, D. A., Fomalont, E. B., Strom, R. G., and Willis, A. G. (1976). Nature **262**, 179.
Bridle, A. H., and Fomalont, E. B. (1978). Astron. J. **83**, 704 (BF).
Burbidge, E. M. (1967). Astrophys. J. **149**, L51.
Burns, J. O., and Owen, F. N. (1977). Astrophys. J. **217**, 34.
Burns, J. O., and Owen, F. N. (1980). Astron. J. **85**, 204.
Colla, G., Fanti, C., Fanti, R., Lari C., Lequeux, J., Lucas, R., and Ulrich, M.-H. (1975). Astron. Astrophys. Suppl. **20**, 1.
Cornwell, T. J., and Wilkinson, P. N. (1981). Mon. Not. R. Astron. Soc. (in press).
Davies, J. G., Anderson, B., and Morison, I. (1980). Nature **288**, 66.
Ekers, R. D., Fanti, R., Lari, C., and Parma, P. (1978). Nature **276**, 588.
Fabbiano, G., Doxsey, R. E., Johnston, M., Schwartz, D. A., and Schwarz, J. (1979). Astrophys. J. **230**, L67.
Fabricant, D., Topka, K., Harnden, F. R., Jr., and Gorenstein, P. (1978). Astrophys. J. **226**, L107.
Fabricant, D., Lecar, M., and Gorenstein, P. (1980). Astrophys. J. **241**, 552.
Gull, S. F., and Northover, K. J. E. (1973). Nature **244**, 80.
Hardee, P. E. (1979). Astrophys. J. **234**, 47.
Harris, A. (1974). Mon. Not. R. Astron. Soc. **166**, 449.
Henriksen, R. N., Vallée, J. P., and Bridle, A. H. (1981). Astrophys. J. (in press) (HVB).
Hjellming, R. M., and Johnston, K. J. (1981). Astrophys. J. (in press).
Högbom, J. A. (1974). Astron. Astrophys. Suppl. **15**, 417.
Högbom, J. A. (1979). Astron. Astrophys. Suppl. **36**, 173.
Högbom, J. A., and Carlsson, I. (1974). Astron. Astrophys. **34**, 341.
Jones, T. W., and Owen, F. N. (1979). Astrophys. J. **234**, 818.
Kotanyi, C. G., and Ekers, R. D. (1979). Astron. Astrophys. **73**, L1.
Linfield, R. (1981). Astrophys. J. **244**, 436.
Lonsdale, C. J., and Morison, J. (1980). Nature **288**, 66.
Miley, G. K. (1976). In *Physics of Nonthermal Radio Sources*, Proceedings of NATO Summer School, edited by G. Setti (Reidel, Dordrecht), p. 1.
Owen, F. N., Burns, J. O., and Rudnick, L. (1978). Astrophys. J. **226**, L119.
Palimaka, J. J., Bridle, A. H., Fomalont, E. B., and Brandie, G. W. (1979). Astrophys. J. **231**, L7.
Perley, R. A., Fomalont, E. B., and Johnston, K. J. (1980). Astron. J. **85**, 649.
Perley, R. A., Fomalont, E. B., and Johnston, K. J. (1981). Astrophys. J. (in press).
Preuss, E., Kellermann, K. I., Pauliny-Toth, I. I. K., and Shaffer, D. B. (1981). Astrophys. J. (in press).
Readhead, A. C. S., and Wilkinson, P. N. (1978). Astrophys. J. **223**, 25.
Rees, M. J. (1978). Nature **275**, 516.
Reich, W., Stute, U., Reif, K., Kalberla, P. M. W., and Kronberg, P. P. (1980). Astrophys. J. **236**, L61.
Sandage, A. (1966). Astrophys. J. **145**, 1.
Schwab, F. R. (1980). 1980 International Computing Conference, SPIE J. **231**, 18.
Stocke J. (1979). Astrophys. J. **230**, 40.
Thompson, A. R., Clark, B. G., Wade, C. M., and Napier, P. J. (1980). Astrophys. J. Suppl. **44**, 151.
Tucker, W. H. (1975). *Radiation Processes in Astrophysics* (MIT, Cambridge), p. 204.
Vallée, J. P., Bridle, A. H., and Wilson, A. S. (1981). Astrophys. J. (in press).
Willis, A. G., Strom, R. G., Bridle, A. H., and Fomalont, E. B.(1981). Astron. Astrophys. **95**, 250.
Wyndham, J. D. (1965). Astron. J. **70**, 384.
Wyndham, J. D. (1966). Astrophys. J. **144**, 459.
Zwicky, F., and Herzog, E. (1963). *Catalogue of Galaxies and of Clusters of Galaxies* (California Institute of Technology, Pasadena), Vol. II, p. 328.